Mon. Not. R. Astron. Soc. **000**, 000–000 (0000) Printed 30 August 2017 (MN LATEX style file v2.2)

On the Galaxy Size–Halo Connection

Andrew Hearin[1], Peter Behroozi[2], Andrey Kravtsov[3], Benjamin Moster[4]
[1] *Argonne National Laboratory, Argonne, IL, USA 60439, USA*
[2] *Department of Physics, University of Arizona, 1118 E 4th St, Tucson, AZ 85721 USA*
[3] *Department of Astronomy & Astrophysics, The University of Chicago, Chicago, IL 60637 USA*
[4] *Universitäts-Sternwarte, Ludwig-Maximilians-Universität München, Scheinerstr. 1, 81679 München, Germany*

30 August 2017

ABSTRACT

We derive empirical modeling constraints on the connection between dark matter halos and the half-mass radius $R_{1/2}$ of galaxy bulges and disks. We show that both $R_{1/2}^{\rm disk}$ and $R_{1/2}^{\rm bulge}$ are well-described by power law scaling relations with halo virial radius, $R_{1/2} = AR_{\rm vir}^{\alpha}$. Novel to this work, we use new SDSS measurements of the $R_{1/2}-$dependence of galaxy clustering to constrain the model parameters, $A_{\rm bulge}, A_{\rm disk}, \alpha_{\rm bulge}, \alpha_{\rm disk}$, and log-normal scatter $\sigma_{R_{1/2}}$. Even when only coarsely tuning these parameters to the observed one-point functions $\langle R_{1/2}^{\rm disk}|M_*^{\rm disk}\rangle$ and $\langle R_{1/2}^{\rm bulge}|M_*^{\rm bulge}\rangle$, our model accurately predicts the observed two-point clustering on small- and large-scales. This success non-trivial, as we show that galaxy clustering is highly sensitive to the physics that shapes satellite galaxy profiles. We find no evidence for the commonly assumed relation between halo spin $\lambda_{\rm halo}$ and $R_{1/2}^{\rm disk}$, and show that this assumption cannot be meaningfully constrained with either the clustering or lensing of L_* galaxies. Our results provide simple boundary conditions for more complex and fine-grained models of galaxy size. We make our python code publicly available to support cosmological surveys that require realistic synthetic galaxy populations.

1 INTRODUCTION

Some introduction goes here.

2 DATA AND SIMULATIONS

2.1 Galaxy Sample

Our galaxy sample comes from Data Release 10 of the Sloan Digital Sky Survey (SDSS Ahn et al. 2014). We study the same M_*-complete galaxy sample used in Behroozi et al. (2015), to which we refer the reader for details. Values for M_* and SFR are taken from the MPA-JHU value-added catalog (Kauffmann et al. 2003; Brinchmann et al. 2004). We cross-match this galaxy sample against the catalog of two-component profile decompositions provided by Meert et al. (2015).

2.2 Clustering Measurements

We calculate two-point clustering $w_{\rm p}$ with line-of-sight projection of $\pi_{\rm max} = 20$Mpc using the `correl` program in `UniverseMachine`.

2.3 Baseline Mock Catalog

2.3.1 Mapping M_* and SFR *to halos*

The starting point of our model is the best-fit `UniverseMachine` model (Behroozi et al. 2017, in prep). This model maps stellar mass and star-formation rate to every halo and subhalo at each snapshot in the Bolshoi-Planck simulation. The stellar mass function, quenched fraction, SFR density, and SFR-dependent clustering are all accurately captured by this model from $z = 0-10$. The model we have developed in the present work does not depend in an essential way upon the `UniverseMachine` model in particular, we only require some reasonably accurate starting point for the M_* and sSFR values mapped to simulated halos.

2.3.2 Mapping B/T *decomposition to halos*

Our model for galaxy size is further predicated upon the mapping between dark matter halos and B/T, the fraction of stellar mass in the bulge. In a companion paper to this work, we will present a separate empirical model for the B/T−halo connection. For our present purposes, we instead rely upon the simplest possible assumption for this connection that recovers the observed distribution $P({\rm B/T}|M_*, {\rm sSFR})$: we suppose that galaxy B/T has no

dependence whatsoever upon halo environment or assembly, beyond what is inherited by the mutual correlation between M_*, sSFR and the cosmic web. That is, we map B/T to dark matter halos by using the M_* and sSFR values from `UniverseMachine` to randomly select the B/T of a galaxy from our SDSS sample with a similar M_* and sSFR. The intuitive interpretation of this modeling choice is that we assume the morphology-density relation is entirely determined by the color-density relation.

3 GALAXY PROFILE MODEL

4 RESULTS

5 DISCUSSION

5.1 Relation to Previous Work

6 CONCLUSION

6.1 Summary

ACKNOWLEDGMENTS

REFERENCES

Ahn C. P., Alexandroff R., Allende Prieto C., Anders F., Anderson S. F., Anderton T., Andrews B. H., Aubourg É., Bailey S., Bastien F. A., et al. 2014, ApJS , 211, 17

Behroozi P., Wechsler R., Hearin A., Conroy C., 2017, in prep.

Behroozi P. S., Zhu G., Ferguson H. C., Hearin A. P., Lotz J., Silk J., Kassin S., Lu Y., Croton D., Somerville R. S., Watson D. F., 2015, MNRAS , 450, 1546

Brinchmann J., Charlot S., White S. D. M., Tremonti C., Kauffmann G., Heckman T., Brinkmann J., 2004, MNRAS , 351, 1151

Hearin A. P., Watson D. F., Becker M. R., Reyes R., Berlind A. A., Zentner A. R., 2014, MNRAS , 444, 729

Kauffmann G., Heckman T. M., White S. D. M., et al., 2003, MNRAS , 341, 33

Meert A., Vikram V., Bernardi M., 2015, MNRAS , 446, 3943

Mo H. J., Mao S., White S. D. M., 1998, MNRAS , 295, 319

Watson D. F., Berlind A. A., Zentner A. R., 2012, ApJ , 754, 90

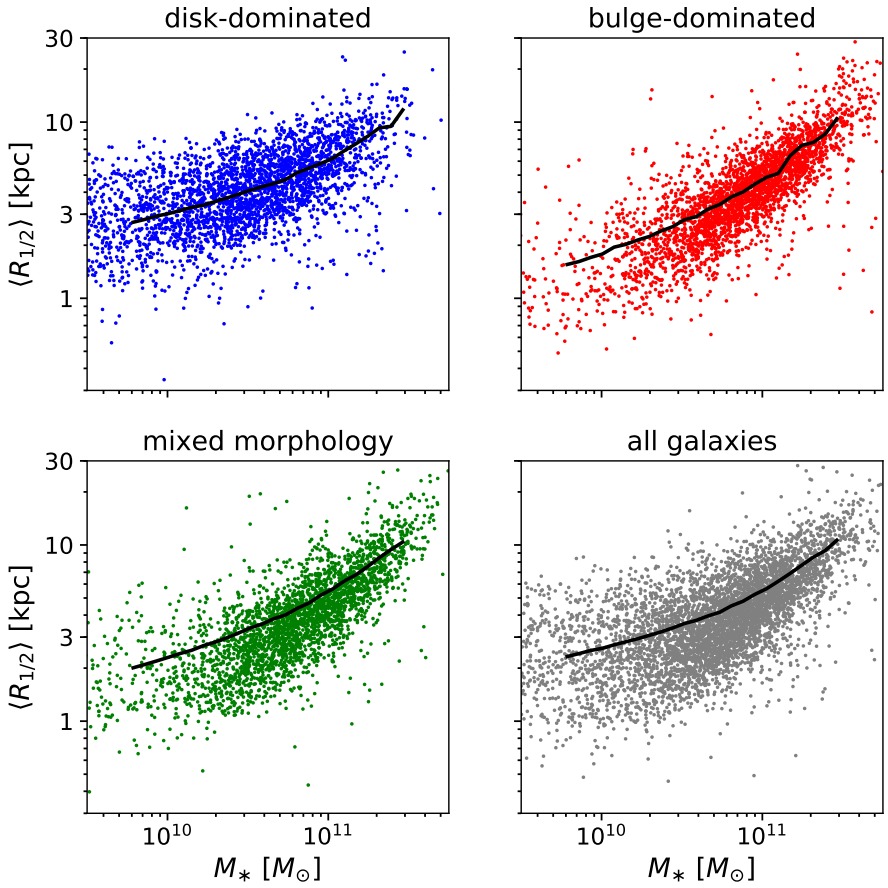

Figure 1. One-point data used to fit the fiducial model. Scattered points show the $R_{1/2} - M_*$ relation for SDSS galaxies as measured in Meert et al. (2015). Bulge-dominated galaxies are defined in terms of the bulge-to-total stellar mass ratio B/T >= 0.75, disk-dominated galaxies B/T < 0.25, mixed morphology as 0.25 < B/T < 0.75. The black curve in each panel shows the $R_{1/2} - M_*$ relation implied by our fiducial model, in which $R_{1/2} = AR_{\rm vir}^{\alpha}$, with $A_{\rm disk} = 0.14 = 7A_{\rm bulge}, \alpha_{\rm disk} = 1, \alpha_{\rm bulge} = 5/4$, and uncorrelated log-normal scatter of 0.2 dex about these relations.

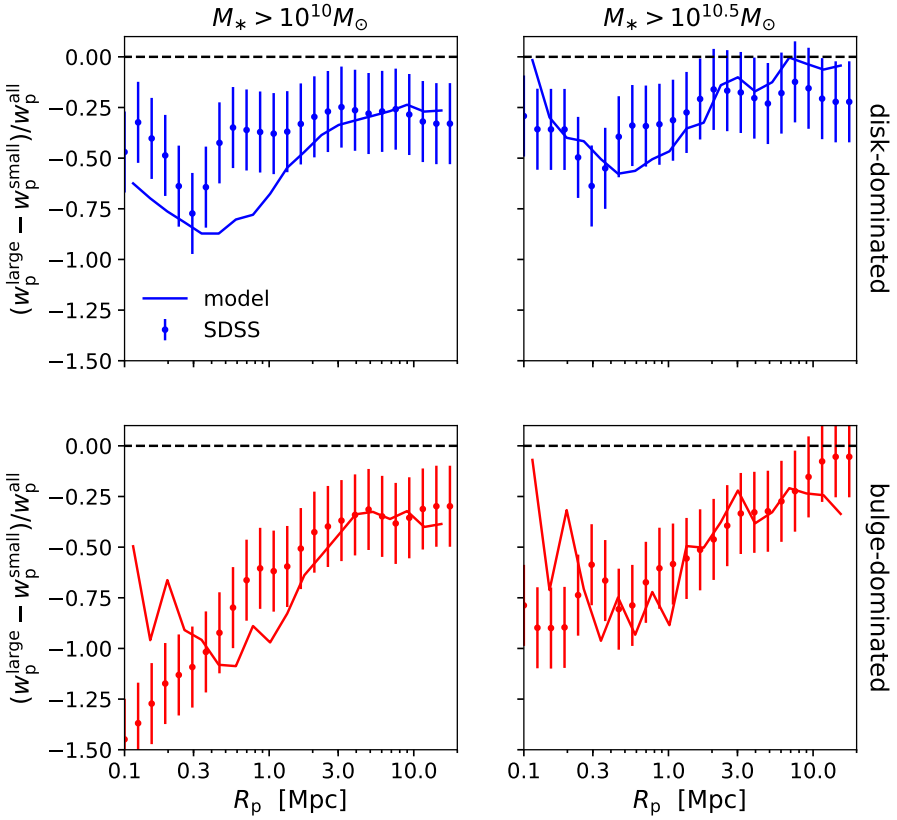

Figure 2. Two-point clustering data used to validate the fiducial model. Points with error bars show new SDSS measurements of the $R_{1/2}-$dependence of projected galaxy clustering, w_p, compared to predictions by the model tuned to the measurements shown in Fig. 1. We define a disk or bulge as "large" or "small" according to whether it is above or below the median size for its stellar mass. The y-axis shows clustering strength ratios, so that, for example, a y-axis value of -0.5 corresponds to small galaxies being 50% more strongly clustered than large galaxies of comparable stellar mass. We show results separately for disk-dominated galaxies (*top* panels) and bulge-dominated galaxies (*bottom* panels), and different thresholds in total stellar mass in the *left* and *right* panels. The successful prediction shown here is remarkable because the model was not fit to these data, and because two-point clustering is highly sensitive to the physics that shapes satellite galaxy profiles (see Fig. 4).

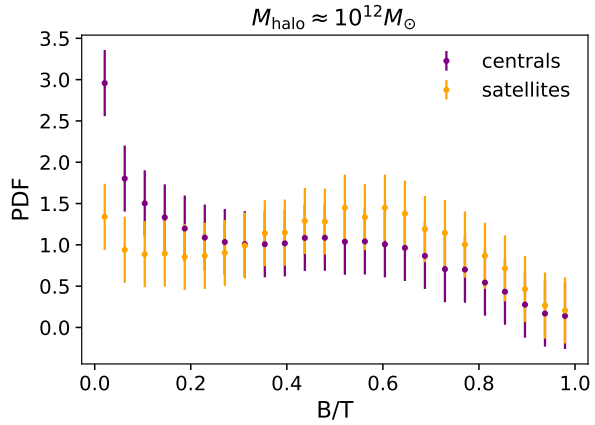

Figure 3. Morphologies of centrals and satellites of the same halo mass. We show the PDF of the bulge-to-total stellar mass ratio B/T of central and satellite galaxies of the same halo mass $M_{\rm halo} = M_{\rm peak}$. In the model, the PDF of B/T is determined by the stellar mass M_* and specific star-formation rate sSFR statistically determine, with no residual dependence on the cosmic web. Satellite galaxies in the model are "bulgier" than centrals of the same halo mass because satellites are more quiescent than centrals of the same stellar mass. Thus our baseline model ansatz is that the morphology-density relation is purely derived from the color-density relation. Since composite size $R_{1/2}$ in the model is given by $R_{1/2} = ({\rm B/T}) R_{1/2}^{\rm bulge} + (1 - {\rm B/T}) R_{1/2}^{\rm disk}$, this ansatz in turn implies that smaller galaxies cluster more strongly relative to larger galaxies of the same stellar mass, as seen in the measurements shown in Fig. 2.

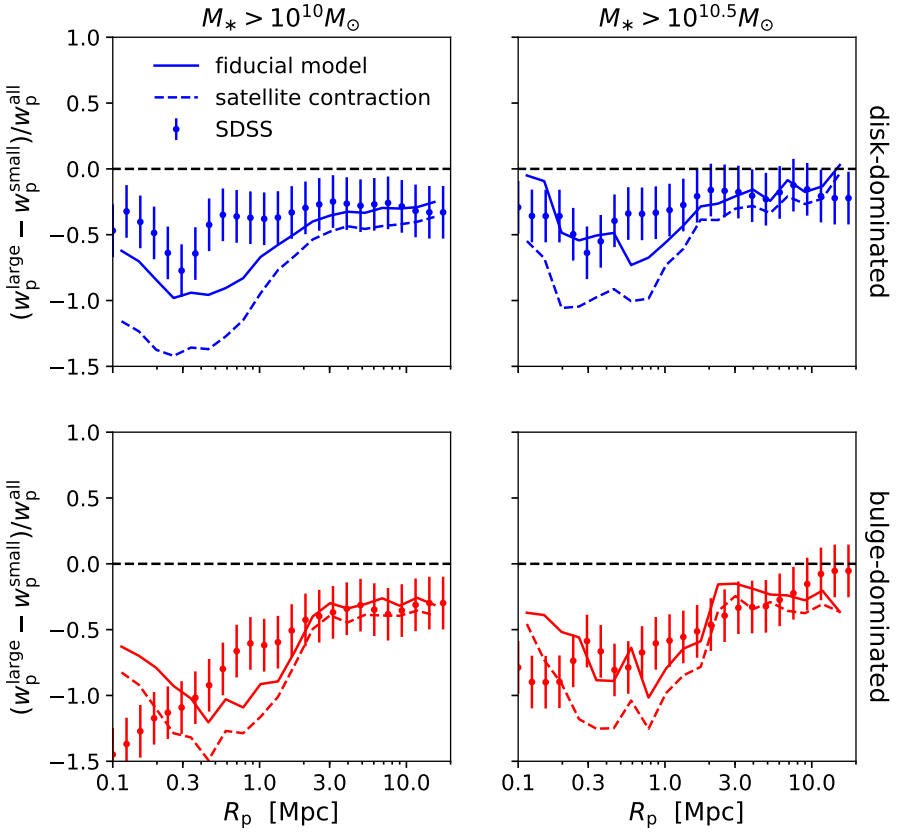

Figure 4. Clustering provides tight constraints on the relative sizes of centrals and satellites. Here we compare our fiducial model, in which satellite galaxy size is set by $R_{\rm vir}$ at the time of infall, to an alternative model analogous to Watson et al. (2012) in which satellite sizes contract in proportion to $(M_{\rm vir}/M_{\rm acc})^{1/3}$. The large differences between solid and dashed curves in the top panels show that the $R_{1/2}-$dependence of galaxy clustering ratios is highly sensitive to the post-infall evolution of satellite galaxy profiles. The successful prediction of our fiducial model, in which satellite galaxies neither contract nor puff up after infall, places tight constraints on satellite-specific physical processes, which must be either negligible or conspiratorially produce little-to-no size change after accretion.

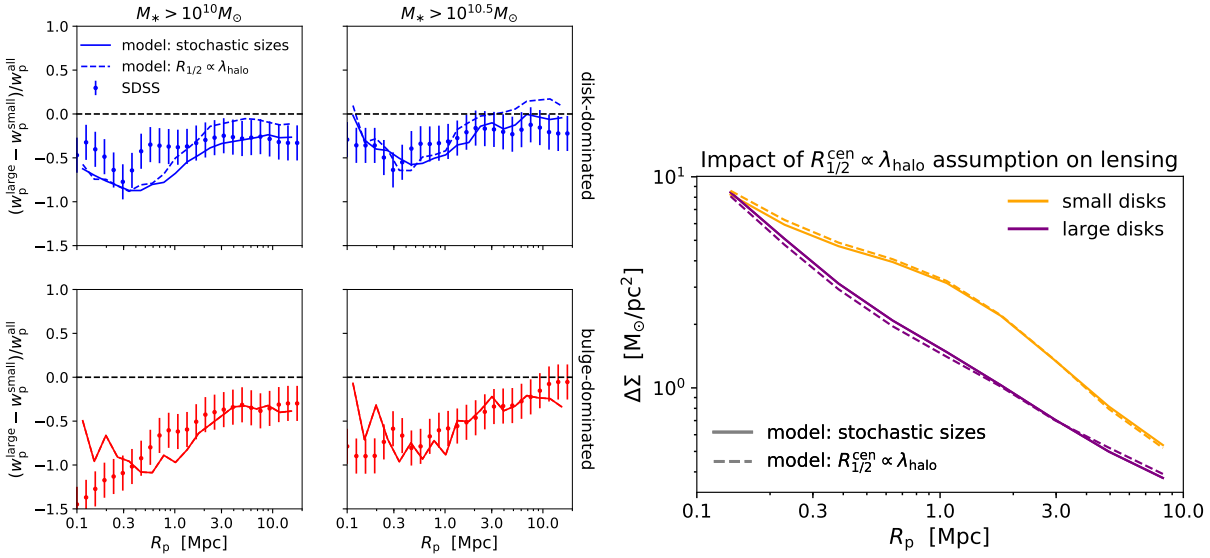

Figure 5. Clustering and lensing provide no constraining power on the assumption that $R_{1/2}^{\rm disk} \propto \lambda_{\rm halo}$. We compare the predictions between our fiducial model in which sizes are purely stochastic, and an alternative model motivated by Mo et al. (1998) in which central galaxy disk size is maximally correlated with host halo spin at fixed stellar mass (implemented via conditional abundance matching, e.g., Hearin et al. 2014). The tiny differences between the solid and dashed curves imply that conventional large-scale structure measurements cannot even in principle provide compelling evidence pertaining to the assumption that $R_{1/2}^{\rm disk} \propto \lambda_{\rm halo}$.